Volumes 113–116 (12 Issues), Spring 2004, ISSN: 0273–2289

Applied Biochemistry and Biotechnology

Biotechnology for Fuels and Chemicals

The Twenty-Fifth Symposium

Editors

Mark Finkelstein
James D. McMillan
Brian H. Davison
Barbara Evans

HUMANA PRESS

0273-2289/04/115/1127–1138/$25.00

Kinetics of Glucose Decomposition During Dilute-Acid Hydrolysis of Lignocellulosic Biomass

Qian Xiang,[1] Yong Y. Lee,[*,1] and Robert W. Torget[2]

[1]Department of Chemical Engineering, Auburn University, Auburn, AL 36849, E-mail: yylee@eng.auburn.edu;
[2]National BioEnergy Center, National Renewable Energy Laboratory, 1617 Cole Boulevard., Golden, CO 80401

Abstract

Recent research work in-house both at Auburn University and National Renewable Energy Laboratory has demonstrated that extremely low concentrations of acid (e.g., 0.05–0.2 wt% sulfuric acid) and high temperatures (e.g., 200–230°C) are reaction conditions that can be effectively applied for hydrolysis of the cellulosic component of biomass. These conditions are far from those of the conventional dilute-acid hydrolysis processes, and the kinetic data for glucose decomposition are not currently available. We investigated the kinetics of glucose decomposition covering pH values of 1.5–2.2 and temperatures of 180–230°C using glass ampoule reactors. The primary factors controlling glucose decomposition are the reaction medium, acid concentration, and temperature. Based on the experimental data, a kinetic model was developed and the best-fit kinetic parameters were determined. However, a consistent discrepancy in the rate of glucose disappearance was found between that of the model based on pure glucose data and that observed during the actual process of lignocellulosic biomass hydrolysis. This was taken as an indication that glucose recombines with acid-soluble lignin during the hydrolysis process, and this conclusion was incorporated accordingly into the overall model of glucose decomposition.

Index Entries: Reaction kinetics; glucose decomposition; dilute acid hydrolysis; kinetic modeling; acid-soluble lignin; acid-base catalysis rules.

Introduction

Saccharification of cellulosic biomass by dilute acid has a much longer history than the enzymatic process. The initial acid-catalyzed wood saccharification was in operation in Germany as early as the 1940s *(1)*. In recent

*Author to whom all correspondence and reprint requests should be addressed.

years, however, treatment of lignocellulosic biomass with dilute H_2SO_4 has been primarily used as a means of pretreatment for enzymatic hydrolysis of cellulose. A concerted research and development effort was phased into the enzymatic hydrolysis process owing to its potential to convert cellulose to glucose nearly quantitatively *(2–3)*. Despite the diminished interest in acid technology, there has been a continual research effort on the subject and a significant advance has also been made in this area *(4)*, including the study of various reactor configurations. The fundamental knowledge and chemistry of biomass processing are still a focus of research interest today. There have also been new developments in kinetic investigations, with the exploration of a broader range of reaction conditions in terms of temperature and acid concentration *(5)*. These activities have contributed to a phenomenal improvement in dilute-acid hydrolysis technology, making it competitive with the enzymatic process *(4)*.

The primary challenge for dilute-acid hydrolysis processes is how to raise glucose yields higher than 70% in an economically viable industrial process while maintaining a high cellulose hydrolysis rate and minimizing glucose decomposition. Percolation reactors have been used in most of the wood sugar processes. Glucose yields of 45–55% and 2–4 wt% sugar concentrations have been generally reported *(1,6–7)*. A significant fraction of the glucan is unaccounted for when the yield is compared with the prediction of percolation process based on two consecutive pseudo-first-order hydrolysis kinetic models developed by Saeman *(8)*. The goal of our research effort was to elucidate the underlying chemistry that limits the yield of glucose in the dilute-acid hydrolysis process.

There have been several improvements to Saeman's original kinetic pattern, and these new models were developed to elucidate the outcomes from actual dilute-acid operations. The explanations for low yields include the following: First, once glucose is formed under reaction conditions, it can be derivatized and/or degraded at a significant rate *(9)*. Second, cellulose has been chemically altered after about 70% conversion *(10)*. Third, 30% of the hydrolyzed cellulose gives rise to oligomers which cannot be converted to glucose *(11)*. These kinetic models predict that glucose yields higher than 65–70% are not attainable using dilute H_2SO_4 for both batch and flow-through type reactors. However, Torget et al. *(12)*, using a simulated countercurrent shrinking-bed reactor system for the aqueous fractionation of yellow poplar, have produced glucose yields higher than 85% by applying 0.07% (w/w) H_2SO_4 and 225°C. The same results have been reproduced in our laboratory. These findings cannot be explained by previously published kinetic models. Further investigation is needed to verify the kinetic pattern and to provide an explanation for the high yields of glucose obtained.

We have therefore studied the kinetics of cellulose hydrolysis and glucose decomposition under extremely dilute H_2SO_4 (0.05–0.2 wt%, pH 1.5–2.2) and high-temperature (200–230°C) conditions. Our ultimate goal is to better understand the kinetics of dilute-acid hydrolysis of biomass and develop promising acid hydrolysis processes that can give both high

glucose yields and sugar concentrations. In the present study, we examined glucose decomposition in both pure solution and hydrolysate liquor medium. An additional pathway for glucose disappearance may exist through the reattachment reaction between glucose and acid-soluble lignin (ASP). In studying "dilute" H_2SO_4 hydrolysis, previous researchers commonly used acid concentration of 0.4 wt% to 1 to 2 wt% *(8,9,13)*. However, those conditions require the use of exotic alloys in the construction of the hydrolysis reactor in order to ensure corrosion resistance. In addition, the higher the acid concentration, the more gypsum is produced owing to lime input for neutralization. The extremely low-acid conditions used in our research work allow the use of lower-cost alloys for the construction of industrial-scale reactors and also reduce the amount of gypsum. Additionally, Zucher-Hammet plots of cellobiose hydrolysis *(14)* and glucose degradation *(15)* indicated that an acid concentration equivalent to a pH (measured at ambient conditions) of 2.2 would favor higher glucose yields.

Materials and Methods

Chemicals and Substrate

All chemicals were purchased from Sigma-Aldrich. d-(+)-Glucose has the product no. G-8270 and lot no. 89H0150, with 99.5% minimum content. α-Cellulose (product no. C8002) contained 92.2% glucan, 3.4% xylan, and 3.2% mannan on dry basis. The ash content was negligible. *Liriodendron tulipifera* L. (yellow poplar) sawdust substrate was provided by the National Renewable Energy Laboratory (NREL) and was used to generate prehydrolysate solution containing ASL. The chemical composition of a representative yellow poplar sample was 42.8 wt% glucan, 14.8 wt% xylan, 2.5 wt% mannan, 0.9 wt% galactan, 0.5% arabinan, 24.3 wt% Klason lignin, 2.8 wt% ASL, and 0.7 wt% ash content based on samples dried at 45°C for over night.

Experimental Apparatus and Procedures

Glucose decomposition studies were conducted in glass ampoule reactors made from 7-mm (Pyrex) glass tubing with a capacity of 2.0 mL. Ampoules were charged with 1 mL of 0.125 *M* glucose solution, sealed, and reacted in a thermostatically controlled bath. The heat transfer tests showed that the contents in the ampoules reached the bath temperature in about 1 min. A correction time of 0.3 min was applied to all the results to compensate for this short warm-up period. After the reaction, the ampoules were quenched in a second bath of cold water, and the contents of the ampoules were collected for analysis by breaking one end and transferring the reacted solutions to vials. The solutions were then analyzed directly by high-performance liquid chromatography (HPLC) for glucose and other components.

Analytical Methods

When aqueous and solid samples were analyzed for moisture and content of sugars, lignin and other chemicals, the procedures described in the NREL Chemical Analysis & Testing Standard Procedure LAP no. 001-014 *(16)* were followed. The analysis of aqueous samples was carried out by two HPLC units: a Bio-Rad (Hercules, CA) Aminex HPX-87P column for analysis of sugars, and a Bio-Rad Aminex HPX-87H column for analysis of acid and other compounds, respectively. Samples were run at 65°C and eluted at 0.6 mL/min with 5 m*M* H_2SO_4 for the HPX-87H column, and 85°C and 0.55 mL/min with pure water for the HPX-87P column.

Results and Discussion

Glucose Decomposition Profile and Rate Constant

Figure 1 shows the profiles of glucose disappearance and the formation of decomposition products at 200°C with an initial pH of 1.8 (0.1 wt% H_2SO_4) and 0.125 *M* concentration of glucose. The major products of glucose decomposition that were identified by HPLC included hydroxymethulfurfural (HMF), 1,6-anhydroglucose, levulinic acid, and formic acid. Other products in the liquor included fructose, cellobiose, acetic acid, humic solid (precipitates), and other gaseous products. When the experimental data for the logarithm of the glucose concentration were plotted with time, a linear relationship was observed. The decomposition rate of glucose at constant temperature and pH is regarded as a pseudo-first-order reaction. Generally, the Arrhenius equation and acid-base catalysis rules are applied to glucose decomposition *(17)*:

$$k^{\mathrm{Glu}} = \left[k_{\mathrm{H_2O}} + k_{\mathrm{H^+}} \times \left(\mathrm{H^+}\right)\ \mathrm{k}_{\mathrm{OH^-}} \times \left(\mathrm{OH^-}\right)\right] \times \exp\left(-\frac{E^{\mathrm{Glu}}}{RT}\right) \qquad (1)$$

in which k^{Glu} is the first-order rate constant for glucose degradation, E^{Glu} is the activation energy, T is the reaction temperature, and R is the gas constant. By acid-base catalysis rules, the preexponential factor comprises three major parts: acid factor (k_{H+}), base factor (k_{OH-}), and solvent factor (k_{H2O}), respectively.

A series of experiments were conducted under various temperatures and pH conditions, and the decomposition profiles were obtained accordingly. The effect of pH on the decomposition is shown in Fig. 2. Surprisingly, the rate of glucose decomposition is found to level off within the pH range of 2.2–7.0, where the decomposition rates are almost identical. This indicates that the solvent term (equal to solvent factor) is the dominance factor of decomposition because the change in pH does not have much of an effect on the overall rate constant. Thus, the acidic term (equal to acid factor times concentration of H^+) has very little effect on overall decomposition, and so does the base term (equal to base factor times OH^-) within this pH range. An SAS nonlinear regression program was then formulated to

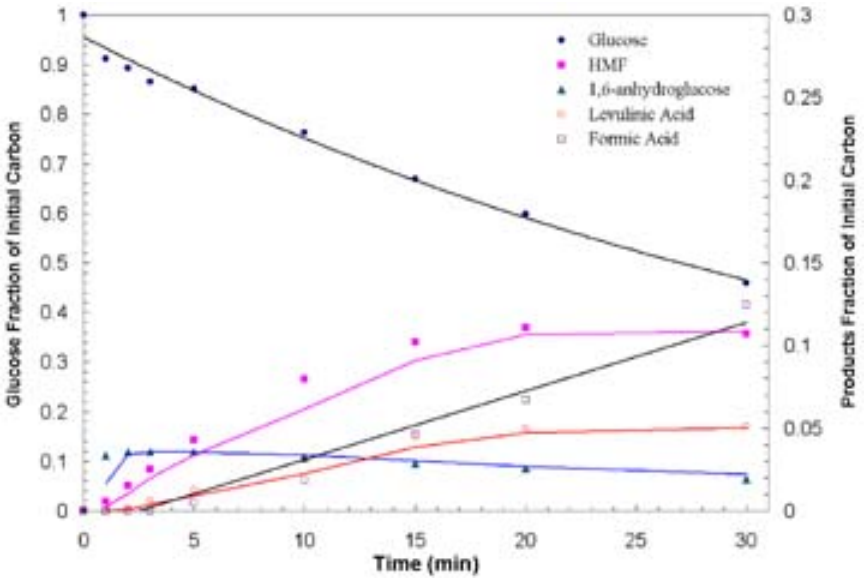

Fig. 1. Profiles of glucose disappearance and formation of decomposition products (under conditions of 200°C, initial 0.125 *M* glucose concentration, and pH 1.8)

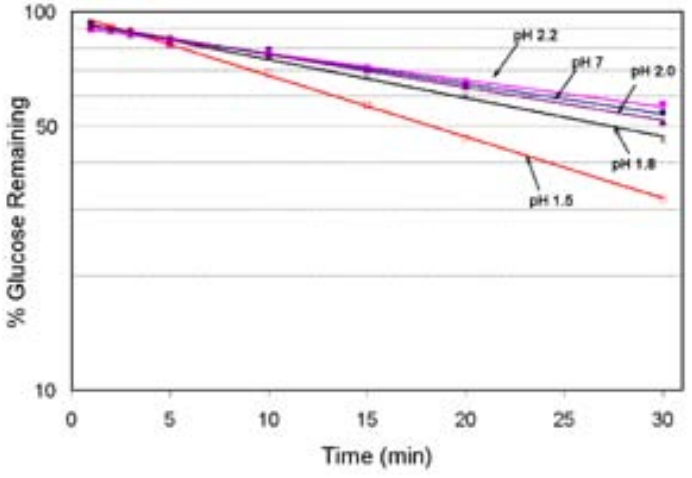

Fig. 2. Profiles and trend lines of glucose decomposition at various pH values and 200°C.

determine the kinetic parameters of Eq. 1 for glucose decomposition in acidic conditions ignoring the effect of OH^- term. The best-fit kinetic parameters give the complete Arrhenius equation in the acidic medium, shown as follows:

$$k^{\mathrm{Glu}} = \left(2.132 \times 10^{13} + 2.148 \times 10^{15} \times 10^{-\mathrm{pH}}\right) \times \exp\left(-\frac{139{,}000}{RT}\right) \qquad (2)$$

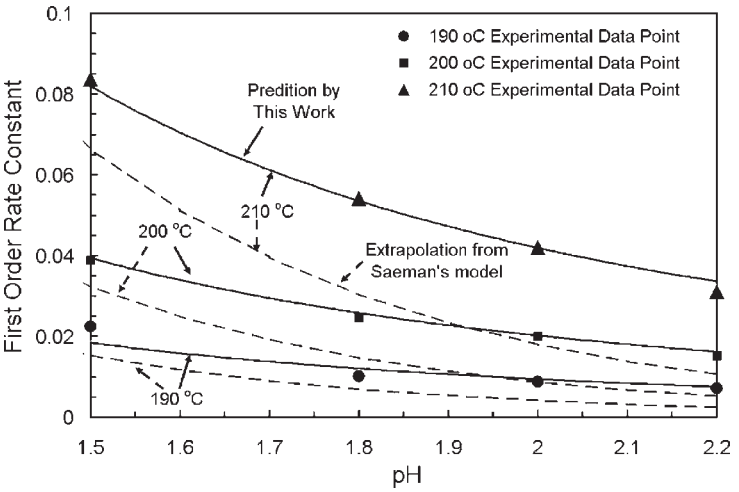

Fig. 3. Rate constants experimentally determined and calculated by proposed model and Saeman's (1945) model under conditions of pH 1.5–2.2 and 190–210°C.

Rate constants (min^{-1}) were calculated by Eq. 2 for given pH values and temperatures. The simulation results were found to be quite consistent with the experimental data as shown in Fig. 3. The estimated activation energy for glucose decomposition, 139 kJ/mol, is consistent with the previously reported data of McKibbins et al. *(17)*, 137 kJ/mol, which was determined from glucose decomposition for a temperature range of 140–250°C and a higher pH region than for our work. At 180–230°C, the glucose decomposition rate approximately doubled for every 10°C increase. Figure 3 also compares the experimental data with the predictions of this model and that of Saeman. The kinetic model developed by this work can accurately predict the first-order rate constants under acidic conditions, especially in extremely low acid concentration ranges (e.g., pH 1.5–2.2). Saeman's model, however, underestimates the rate constants because it ignores the solvent term in decomposition kinetics. When acid concentration is increased (pH is decreased), the trend lines of the two kinetic models eventually merged. This means that the solvent term is less important than the acid term and can thus ignored at high acid concentration range, which is what Saeman's model assumed.

Reversible Reaction in Glucose Decomposition

From the experimental results in Figs. 1 and 2, the first-order reaction trend lines could not be traced back to the origin (time at 0 and a glucose fraction at 1) on extrapolation. This phenomenon can be observed in most previously reported data. It indicates that the reversible reactions are much faster than irreversible glucose decomposition and equilibrium is attained at early phase of the reaction. Conner et al. *(9)* suggested an

extended kinetic model for glucose decomposition and cellulose hydrolysis that incorporates the reversible reactions of glucose.

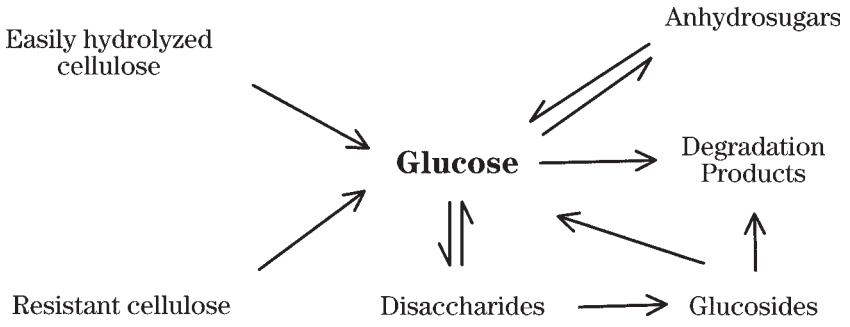

Conner's Hydrolysis Model

A complicated mathematic model was also developed for cellulose saccharification that includes glucose decomposition, reversible reactions, and disaccharide dehydration. With the implementation of the modified kinetic model, such as inclusion of the reversible reactions with 1,6-anhydrosugars and disaccharides, the fit of experimental data to the predicted model has been greatly improved. A number of researchers who have conducted mechanistic studies of glucose reactions in aqueous solutions found that the isomerization of glucose to fructose (and mannose) was found to be an important reaction pathway, especially under extremely low acid or pure-water conditions *(18)*. Fructose itself is also subject to decomposition and other reversible reactions after being formed from glucose through the reversible isomerization reactions. If one adds these reversible isomerization reaction pathways to the kinetic model in the above scheme, along with the decomposition of the fructose pathway, a more complicated kinetic model is expected.

Assuming that the glucose decomposition reaction (excluding all reversible reactions) follows first order kinetics, certain conclusions can be drawn from the glucose residual profiles of the actual experimental data. First, the overall reversible reactions, including isomerization and dehydration, have a much greater reaction rate than glucose decomposition, and equilibrium is reached at the early phase of the reaction. Second, straight lines are obtained once the equilibria are established. This indicates that the components produced from the reversible reaction are also subject to decomposition, which occurs at approximately the same reaction rate level as glucose decomposition. This ensures the first-order reaction nature of the decomposition reaction. Third, acid concentration and temperature will affect both the glucose decomposition rate and the reversible reactions rate. Based on these conclusions, we propose a simplified mathematical model for the glucose decomposition mechanism, which is discussed in the next section.

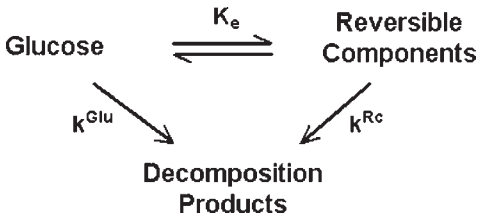

Fig. 4. Simplified kinetic model for glucose decomposition.

Kinetic Model for Glucose Decomposition Involving Reversible Reactions

Figure 4 shows the scheme of a simplified kinetic model for glucose decomposition involving reversible reactions. It was developed based on following assumptions: First, all reversible reactions are combined into one reaction with a single equilibrium constant, K_e. Second, since the reversible reaction is very rapid, equilibrium is attained instantly. Third, reversible components are also subject to degradation at the same rate level as glucose. Therefore, the reversible reaction does not affect the first-order reaction pattern of glucose disappearance once the equilibrium is established. Fourth, both the rate constant k^{Glu} and equilibrium constant K_e are functions of pH and temperature. In acidic conditions, they are governed by both Arrhenius equation and general acid-base catalysis rules. Therefore, reaction kinetics are expressed by the following equations, omitting the term for hydroxyl ion (OH^-) under the acidic conditions:

$$k^{\mathrm{Glu}} = \left[K_{\mathrm{H_2O}} + K_{\mathrm{H^+}}\left(\mathrm{H^+}\right)\right] \times \exp\left(-\frac{E^{\mathrm{Glu}}}{RT}\right) \tag{3}$$

$$k_e = \left[K_{e_{\mathrm{H_2O}}} + K_{e_{\mathrm{H^+}}}\left(\mathrm{H^+}\right)\right] \times \exp\left(-\frac{\Delta H}{RT}\right) \tag{4}$$

And the glucose profile is expressed from the model as follows:

$$\frac{\mathrm{Glu}}{\mathrm{Glu}_0} = \frac{\exp\left(-K^{\mathrm{Glu}} \times t\right)}{\left(1 + K_e\right)} \tag{5}$$

in which Glu_0 is the initial glucose concentration. Best-fit kinetic parameters within the pH range of 1.5–2.2, as determined by SAS nonlinear regression analysis, are as follows:

$$k^{\mathrm{Glu}} = \left[2.132 \times 10^{13} + 2.148 \times 10^{15} \times \left(\mathrm{H^+}\right)\right] \times \exp\left(\frac{-139{,}000}{RT}\right) \tag{6}$$

$$k_e = \left[1.2531 - 35.37 \times \left(\mathrm{H^+}\right)\right] \times \exp\left(\frac{-10{,}640}{RT}\right) \tag{7}$$

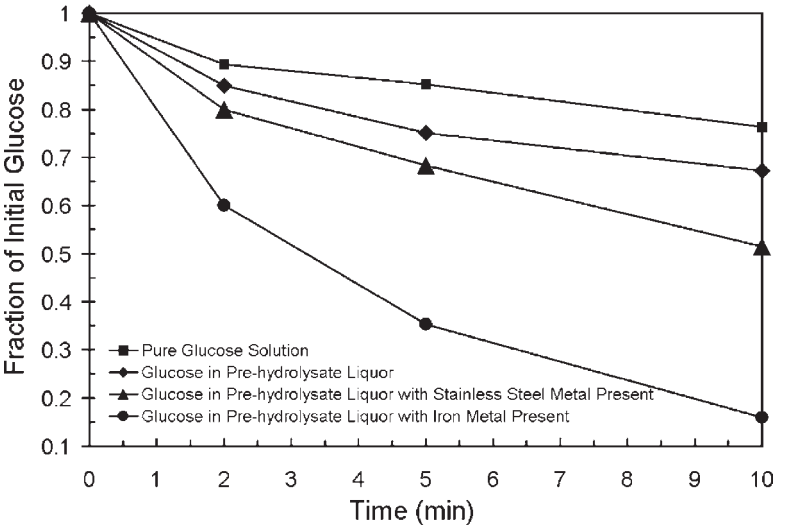

Fig. 5. Glucose decomposition affected by presence of ASL and by presence of metals.

This model includes the reversible reaction pathways, which predict the glucose decomposition behavior better than the pseudo-first-order kinetic model, especially when both pH and temperature are high. Because of the reversible decomposition reactions, under the conditions applied in this investigation (200°C and pH 1.5–2.2) and with the use of percolation or shrinking-bed reactors, this model predicts that there is 4–8% glucose loss owing to reversible reactions (after liberation from biomass). We note that the kinetic parameters determined in this work may not be applied to high pH region.

Other Factors Affecting Glucose Decomposition

To study how other factors affect glucose decomposition during the biomass hydrolysis process, reaction media are made up with biomass-prehydrolysis liquor, which contains ASL, to simulate glucose decomposition of lignocellulosic biomass. The results are summarized in Fig. 5. The data indicate that glucose undergoes faster decomposition in prehydrolyzed acidic liquor than in pure acidic medium. We believe that this is caused by an additional glucose degradation pathway through a recombination reaction with ASL. Additional evidence for this is presented in our previous research *(19)*. With ASL in the acidic medium, the presence of protons causes formation of reactive intermediates of various types such as protonized glucose. They would have high affinity for any positively charged molecules including nucleophilic reaction partners. This system is primarily involved as a reaction partner in lignin fragmentation or lignin condensation reactions, depending on the type of the

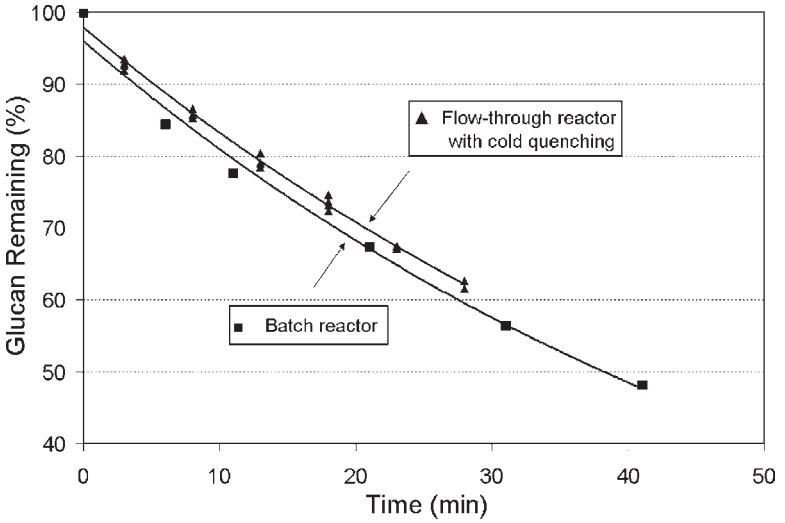

Fig. 6. Comparison of hydrolysis of α-cellulose at 205°C, pH 2.2 between batch and flow-through reactors.

active nucleophile *(20)*. Thus, the active sites on ASL will lead to the combination reaction between ASL and glucose or oligomers as follows:

$$\text{ASL} + \text{Glucose} \rightarrow \text{ASL-Glucose}$$
$$\text{ASL} + \text{Oligomer} \rightarrow \text{ASL-Oligomer}$$

This provides an explanation for the unaccounted glucose loss during the acid hydrolysis process. It also gives an explanation for the generally low yield for dilute acid hydrolysis processes and previously unclosed carbon mass balance.

More evidence exists for the combination of glucose with ASL. After comparing the hydrolysis performance in different reactor systems, Torget et al. *(21)* reported that the observed kinetics of biomass hydrolysis could be much different for various reactor configurations, and the difference is indeed phenomenal. A flow-through reactor with yellow poplar as feedstock exhibits a hydrolytic reaction rate two to three times that of a batch reactor, whereas about two-thirds of the total lignin is dissolved into the liquid during both types of processing. However, when nonlignin feedstocks such as α-cellulose are subjected to the same comparison, very little difference in hydrolysis rate is found as shown in Fig. 6. The rate constants are 0.0171 min^{-1} for the batch reactor and 0.0162 min^{-1} for the flow-through reactor under the same hydrolysis conditions. The principal molecular mechanism of acid-catalyzed hydrolysis of cellulose (cleavage of β-1-4-glycosidic bond) has been described to proceed in three steps. The reaction starts with a proton from the acid interacting rapidly with the glycosidic oxygen linking two sugar units, forming a conjugate acid. The cleavage of the C–O bond and breakdown of the conjugate acid to the

cyclic carbonium ion then takes place, which adopts a half-chair conformation. After a rapid addition of water, free sugar and a proton are liberated *(22–25)*. The formation of the intermediate carbonium ion takes place more rapidly at the end than in the middle of the polysaccharide chain. When ASL is presented in the reaction medium at high temperature, it combines with oligomers at the reducing end, thus preventing the formation of such carbonium ion. The hydrolysis rate with yellow poplar in a batch reactor is therefore slowed down. The lignin can be effectively removed in a flow-through reactor and a higher hydrolysis rate is obtained. Since α-cellulose does not contain lignin, the exhibited hydrolysis rates are identical in both batch and flow-through reactors under the same conditions.

Experimental runs have also been conducted in the presence of different metals to demonstrate how various metals for the construction of industrial hydrolysis reactors may affect the overall degradation of glucose during the real process of biomass dilute-acid hydrolysis. The glucose decomposition profiles in the presence of stainless steel (S.S.) and iron are also presented in Fig. 5. Comparing four different metals, we found that copper and Hastelloy C-276 have very little effect on glucose decomposition, whereas stainless steel has a significant effect. Most notably, iron has the strongest impact on glucose decomposition, causing a very fast disappearance of residual glucose in the reaction medium.

Conclusion

The kinetic pattern for glucose decomposition is affected by many factors, including the reaction medium, reactor configuration, and temperature. Based on glucose decomposition kinetic data obtained from glass ampoule reactors, a simplified kinetic model was developed taking all reversible pathways into consideration. The best-fit parameters were determined by nonlinear regression analysis. However, the glucose decomposition rate in actual hydrolysis processes is found to be faster than the predictions based on the kinetic model obtained from ampoule glass reactors. A new pathway for glucose disappearance through a combined reaction between glucose and ASL is believed to be partly responsible for previously unaccounted for glucose decomposition. Metal and/or metal ions can also catalyze glucose decomposition; thus, the material used in the construction of reactor must be carefully selected.

The kinetic model established by our work can accurately predict the rate constants of glucose decomposition over a broad range of acid concentrations including extremely low acid conditions (pH 1.5–2.2) in which Saeman's model fails to hold.

Acknowledgments

This research was sponsored by the US Department of Energy under Cooperative Agreement DE-FC36-01GO11072, and by National Renewable Energy Laboratory under subcontract ACO-1-31003-01.

References

1. Faith, W. L. (1945), *Ind. Eng. Chem. Res.* **37,** 1–9.
2. Wyman, C. E. (1994), *Bioresour. Technol*. **50,** 3–16.
3. van Walsum, P., Allen, S. G., Laser, M. S., Spencer, M. J., Antal, M. J., and Lynd, L. R. (1996), *Appl. Biochem. Biotechnol*. **57/58,** 157–170.
4. Lee, Y. Y., Iyer, P., and Torget, R. W. (1999), *Adv. Biochem. Eng.* **65,** 93–115.
5. Torget, R. W., Hayward, T. K., Hatzis, C., and Philippidis, G. P. (1995), in *17th Symposium on Biotechnology for Fuels and Chemicals*, Vail, Co.
6. Gilbert, N. G., Hobbs, I. A., and Levine, J. D. (1952), *Ind. Eng. Chem.* **44,** 1712.
7. Harris, E. E. (1949), *Adv. Carbohydr. Chem.* **4,** 153–188.
8. Saeman, J. F. (1945), *Ind. Eng. Chem. Res*. **37,** 43–52.
9. Conner, A. H., Wood, B. F., Hill, C. G., and Harris, J. F. (1986), in *Cellulose: Structure, Modification and Hydrolysis*, Young, R. A. and Rowell, R. M., eds., John Wiley and Sons, New York, NY, pp. 281–296.
10. Bouchard, J., Abatzoglou, N., Chornet, E., and Overend, R. P. (1989), *Wood Sci. Technol*. **23,** 343–355.
11. Mok, W. S., Antal, M. J., and Varhegyi, G. (1992), *Ind. Eng. Chem. Res.* **31**, 94–100.
12. Torget, B., Nagle, N., Hayward, T. K., and Elander, R. (1997), in *19th Symposium on Biotechnology for Fuels and Chemicals,* Colorado Springs, CO.
13. Harris, J. F., Baker, A. J., Connor, A. H., Jeffries, T. W., Minor, J. L., Pettersen, R. C., Scott, R. C., Springer, E. L., Wegner, T. H., and Zerbe, J. L. (1985), *General Technical Report FPL-45*, US Department of Agriculture Forest Products Laboratory, Madison, WI.
14. Bobleter, O., Schwalk, W., Concin, R., and Binder, H. (1986), *J. Carbohyd. Chem*. **5(3),** 387–399.
15. Popoff, T. and Theander, O. (1976), *Acta Chem. Stand.* **30,** 397–402.
16. Ehrman, C., Ruiz, R., Templeton, D., Adney, W. S., Baker, J. D., and Hsu, D. (1995), *Chemical Analysis & Testing Standard Procedure, LAP no. 001–014*, National Renewable Energy Laboratory, Golden CO.
17. McKibbins, S. W., Harris, J. F., Saeman, J. F., and Neill, W. K. (1962), *Forest Prod. J.* **12,** 17.
18. Kabyemela, B. M., Adschiri, T., Malaluan, R. M., and Arai, K. (1999), *Ind. Eng. Chem. Res.* **38(8),** 2888–2895.
19. Xiang, Q., Kim, J. S., and Lee, Y. Y. (2003), *Appl. Biochem. Biotechnol*. **105–108,** 337–352.
20. Fengel, D. and Wegener, G. (1984), *Wood—Chemistry, Ultrastructure, Reactions*. Walter de Gruyter, Berlin, Germany.
21. Torget, R. W., Kim, J. S., and Lee, Y. Y. (2000), *Ind. Eng. Chem. Res.* **39,** 2817–2825.
22. Shafizadeh, F. (1963), *TAPPI* 46, 381–383.
23. Timell, T. E. (1964), *Can. J. Chem. 42*, 1456–1472.
24. Harris, J. F. (1975), *Appl. Polym. Symp*. **28,** 131–144.
25. Philipp, B., Jacopian, V., Loth, F., Hirte, W., and Schulz, G. (1979), in *Hydrolysis of Cellulose: Mechanisms of Enzymatic and Acid Catalysis*, Adv. Chem. Ser. 181, Brown, Jr. R. D. and Jurasek, L., eds., American Chemical Society, Washington, DC, pp. 127–143.

National Renewable Energy Laboratory

PERMISSION TO USE COPYRIGHTED MATERIAL

PERMISSIONS

I give the National Renewable Energy Laboratory (NREL) of Golden, Colorado, irrevocable and worldwide permission to post the following onto its site on the World Wide Web (Web).

☒ Yes
☐ No

Name of document, report, article, etc.: Eight U.S. Department of Energy Biomass Program (NREL, ORNL, ANL, INEEL, PNNL) authored articles from 25th Symposium on Biotechnology for Fuels and Chemicals, Breckenridge, CO, May 2003 — Applied Biochemistry and Biotechnology, Volumes 113-116, Spring 2004, ISSN 0273-2289 pp. 13-26, 113-114, 653-670, 807-826, 871-886, 1127-1138, 1139-1162, 1163-1166.

In addition to posting on the Web, I give NREL worldwide permission to distribute hard copies of the document in response to requests.

☒ Yes
☐ No

*****PLEASE NOTE*****

- For jointly authored works, only one signature is required, but we assume all authors have been advised and have consented to the terms of this form.
- If you are employed and you prepared your work as a part of your job, the rights to your work initially rest with your employer. In that case, when you sign this form, we assume you are authorized to do so by your employer and that your employer has consented to the terms and conditions of this form. If not, it should be signed by someone so authorized.

When posting on the Web, NREL will credit the copyright holder thus: **Posted on this site with permission from** Humana Press

When distributing hard copies, NREL will label the document: **Reprinted with permission from** Humana Press

☐ I was a U.S. government employee when I produced this work as part of my federal employment and therefore the work is not subject to U.S. copyright protection.

☐ I deny permission to post the document on the Web or to distribute hard copies, but give permission for the document to be abstracted and cited in NREL's database, along with information about obtaining the document directly from the copyright holder.

The document can be obtained by writing:

SIGNATURE

I represent and warrant that I have the full right and authority to grant the rights herein granted, that no one else's permission is required, and that should my work contain previously published and/or copyrighted material that permission has been obtained for such use and that any required credit lines and copyright notices are duly noted.

Thomas B Lanigan
Printed name

Vice President, Humana Press
Title and Company

Thomas B Lanigan
Signature

5/27/04
Date